THE JOURNAL OF PHYSICAL CHEMISTRY A

Article

pubs.acs.org/JPCA

Complex Frequency-Dependent Polarizability through the $\pi \rightarrow \pi^*$ Excitation Energy of Azobenzene Molecules by a Combined Charge-Transfer and Point-Dipole Interaction Model

Shokouh Haghdani, Nazanin Davari, Runar Sandnes, and Per-Olof Åstrand*

Department of Chemistry, Norwegian University of Science and Technology (NTNU), N-7491 Trondheim, Norway

ABSTRACT: The complex frequency-dependent polarizability and $\pi \rightarrow \pi^*$ excitation energy of azobenzene compounds are investigated by a combined charge-transfer and point-dipole interaction (CT/PDI) model. To parametrize the model, we adopted time-dependent density functional theory (TDDFT) calculations of the frequency-dependent polarizability extended with excited-state lifetimes to include also its imaginary part. The results of the CT/PDI model are compared with the TDDFT calculations and experimental data demonstrating that the CT/PDI model is fully capable to reproduce the static polarizability as well as the $\pi \rightarrow \pi^*$ excitation energy for these compounds. In particular, azobenzene molecules with different functional groups in the *para*-position have been included serving as a severe test of the model. The $\pi \rightarrow \pi^*$ excitation is to a large extent localized to the azo bond, and substituting with electron-donating or electron-attracting groups on the phenyl rings results in charge-transfer effects and a shift in the excitation energy giving rise to azobenzene compounds with a range of different colors. In the CT/PDI model, the $\pi \rightarrow \pi^*$ excitation in azobenzenes is manifested as drastically increasing atomic induced dipole moments in the azo group as well as in the adjacent carbon atoms, whereas the shifts in the excitation energies are due to charge-transfer effects.

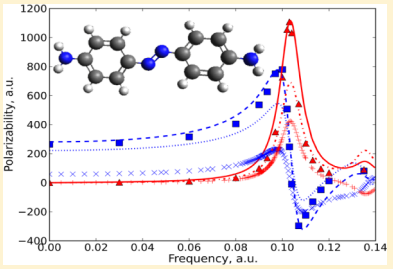

I. INTRODUCTION

The most important characteristic of azo compounds is as color dyes.[1−4] Due to the importance of azo compounds in nonlinear optical materials, photophysical characteristics of azo compounds have also been studied extensively,[5−14] and the suitable laser wavelengths to obtain a *trans* to *cis* isomerization in azobenzene dyes have been studied theoretically.[10,11,15−17] The isomerization occurs by either n $\rightarrow \pi^*$ or $\pi \rightarrow \pi^*$ transitions where n, π, and π^* denote the highest occupied lone-pair orbital, the highest occupied π orbital, and the lowest unoccupied π orbital, respectively.[18−20] The intensity of the n $\rightarrow \pi^*$ transition is however small due to symmetry reasons and therefore the $\pi \rightarrow \pi^*$ excitation is the most important.[18] The excitation energy of $\pi \rightarrow \pi^*$ transitions can be reduced by electron-donating and/or electron-accepting substituents in the azobenzene molecule[11,21,22] or by replacing one of the phenyl rings by for example a thiazole unit.[23,24]

The frequency-dependent molecular polarizability is a measure of the response to a time-dependent electric field which is fundamental in the construction of electrical and optical devices by means of molecules.[25,26] The molecular polarizability is often investigated by time-dependent density functional theory (TDDFT).[27−30] The polarizability greatly enhances near resonance frequencies[31] and the maximum values of the imaginary part of the polarizability as a function of frequency are related to the excitation energies and the UV/vis absorption spectrum. The excitation energies can therefore be calculated by two different approaches: by response theory analyzing the poles of the frequency-dependent polarizability[32] and by the frequency-dependent polarizability with an imaginary term describing the lifetime of the excited state.[33,34]

Force-fields represent an alternative method for larger molecular systems to obtain the system response properties such as the polarizability.[35] In this work, we adopt a force-field model,[36] which consists of a combination of a nonmetallic charge-transfer/point-dipole interaction (CT/PDI) model[37] and a model for the frequency-dependent polarizability.[38]

In the electronegativity equalization model (EEM),[39,40] an atomic electronegativity and an atomic chemical hardness, which are regarded as atom-type parameters, describe the charge flow between atoms. The atomic charges are redistributed so that the electronegativity (chemical potential for electrons) is equal throughout the molecule. The reformulation of EEM by the atom−atom charge transfer (AACT) method[41] gives the energy in terms of charge-transfer variables, and it was used to modify the model by adding an extra energy term for the polarizability to scale correctly with the size of a nonmetallic system.[37] It has been noted for a long time that the EEM is in principle a metallic model,[41,42] for example a water model has been constructed where charge-transfer between the water molecules is not allowed by adding extra constraints.[40,43] Modifications to the EEM have been suggested to resolve this problem,[37,41,44−51] and the modified models have also been connected to DFT.[52−55]

Received: July 29, 2014
Revised: October 22, 2014
Published: October 30, 2014

   dx.doi.org/10.1021/jp507639z | *J. Phys. Chem. A* 2014, 118, 11282−11292

In the point-dipole interaction (PDI) model,[56−60] the molecular polarizability is obtained by solving a set of coupled linear equations for a system of atomic polarizabilites. The coupling occurs due to the interaction of atomic induced dipole moments in an external electric field, and the atomic polarizabilites are considered as atom-type parameters in this model. The PDI model has been employed extensively for the calculations of polarizabilities of large systems,[61−63] and it has been extended to other response properties like hyperpolarizabilities,[35,64−70] optical rotation,[71−74] and Raman intensities.[75,76]

The PDI model has been combined with the EEM[77−82] and also with a similar capacitance model.[42,83−86] In the combined charge-transfer and PDI model employed in this work,[36,37] a Gaussian distribution is adopted for each atom instead of a point-charge.[87,88] The methodology has been extended to the frequency-dependent polarizbility,[38] and the combined method has been successfully used to study the frequency-dependent polarizability of alkanes, polyenes, and aromatic systems[36] but did not include excitation energies and was thereby restricted to the frequency-dependence far away from absorption.

Using the CT/PDI model,[36] we calculate here the frequency-dependent polarizability including the $\pi \rightarrow \pi^*$ excitation energy of a set of *trans*-azobenzene molecules with different functional groups at the *para*-position. By studying a group of azobenzene molecules, we investigate in particular the sensitivity of the coupling between the charge-transfer and the point-dipole terms. The $\pi \rightarrow \pi^*$ excitation in azobenzene is essentially localized to the azo-bond, but the excitation energy is sensitive to the addition of functional groups in the phenyl rings.[10,11,21,22,89,90] The functional groups are either electron-donating or electron-withdrawing causing electron transfer to or from the azo group inducing a shift in excitation energy. As found here, it is the atomic dipole term in the azo group (and the adjacent carbon atoms) that becomes large at absorption, but their frequency-dependence is adjusted by charge-transfer from the functional groups through the phenyl rings. Azobenzenes with various substitutions are thus a sensitive and supposedly challenging test for a force-field model to describe molecular electronic excitations. We have used the TDDFT[27−30] method to compute reference data for the frequency-dependent polarizability, and we parametrize our model using the obtained DFT reference data and finally compare the results of our model to DFT and experimental results.

The paper is organized as follows. In section II, we discuss the model employed to study the azo compounds. In section III, we present the parametrization method along with the obtained parameters. In section IV, the results are analyzed and compared with DFT and experiments. Finally in section V, we summarize our results and give concluding remarks.

II. THEORETICAL MODEL

The CT/PDI model is presented in detail in ref 36, and here we only summarize the model. In the CT/PDI model, the frequency-dependent polarizability is obtained by a combination of a nonmetallic electronegativity equalization and a point-dipole interaction model.[36−38] In the time-dependent charge-dipole model,[38] each atom is associated with a time-dependent charge $q_I(t)$ and a time-dependent dipole moment $\mu_I(t)$. The atomic charges $q_I(t)$ can be recast by means of charge-transfer variables $q_{IK}(t)$ so that in a system containing N particles[36]

$$q_I(t) = \sum_K^N q_{IK}(t) \tag{1}$$

The Lagrange equations including the kinetic energies for $q_{IK}(t)$ and $\mu_I(t)$ as well as the potential energy provide a set of coupled linear equations. Finally, the frequency-dependent polarizability is calculated using the solutions to these linear response equations, which provides the corresponding frequency-dependent atomic properties $q_{IK}(\omega)$ and $\mu_I(\omega)$.[36] The Lagrangian, L, of the system can be expressed by[38]

$$L = K^q + K^\mu - V \tag{2}$$

where K^q and K^μ are the kinetic energies of atomic charges and atomic dipole moments, respectively, whereas V is a potential energy. The kinetic energy K^q associated with the oscillations of charges is in our model given by[36]

$$K^q = \frac{1}{2}\sum_{I,K>I}^N (c_I^{q*} + c_K^{q*}) R_{IK}^2 (\dot{q}_{IK})^2 \tag{3}$$

in which R_{IK} is the bond distance between atoms I and K, and $\dot{q}_{IK}$ is the time-derivative of q_{IK}. Here c_I^{q*} and c_K^{q*} are atom-type parameters. The kinetic energy K^μ of the oscillating atomic dipole moments is analogously given as[38]

$$K^\mu = \frac{1}{2}\sum_I^N c_I^{\mu*} (\dot{\mu}_I)^2 \tag{4}$$

where $\dot{\mu}_I$ is the time derivative of μ_I, and $c_I^{\mu*}$ is an additional atom-type parameter. The potential energy in eq 2 contains three terms[37]

$$V = V^{qq} + V^{q\mu} + V^{\mu\mu} \tag{5}$$

where V^{qq} is the charge−charge interaction, $V^{q\mu}$ is the charge-dipole interaction and $V^{\mu\mu}$ is the dipole−dipole interaction energy. The charge−charge term is[78,79]

$$V^{qq} = \sum_I^N (\chi_I^* + \varphi_I^{\text{ext}}) q_I + \frac{1}{2}\eta_I^* q_I^2 + \frac{1}{2}\sum_{I\neq J}^N q_I T_{IJ}^{(0)} q_J \tag{6}$$

where χ_I^* and η_I^* are atom-type parameters which introduce the atomic electronegativity and atomic chemical hardness, respectively, whereas φ_I^{ext} is the external electrostatic potential at atom I. In classical electrostatics $T_{IJ}^{(0)} = 1/R_{IJ}$ where R_{IJ} is the distance between atoms I and J. Hence, $q_I T_{IJ}^{(0)} q_J$ is the Coulomb interaction. In the CT/PDI model, V^{qq} is rewritten in terms of charge-transfer variables in eq 1 as[37]

$$V^{qq} = \sum_{I,K>I}^N (\chi_{IK} + \varphi_{IK}^{\text{ext}}) q_{IK} + \frac{1}{2}\sum_{I,K>I,J,M>J}^N q_{IK} T_{IK,JM}^{(0)} q_{JM} \tag{7}$$

where $T_{II}^{(0)} = \eta_I^*$, $\chi_{IK} = \chi_I^* - \chi_K^*$, $\varphi_{IK}^{\text{ext}} = \varphi_I^{\text{ext}} - \varphi_K^{\text{ext}}$ and

$$T_{IK,JM}^{(0)} = T_{IJ}^{(0)} - T_{KJ}^{(0)} - T_{IM}^{(0)} + T_{KM}^{(0)} \tag{8}$$

Several modifications to $T_{IK,JM}^{(0)}$ are utilized. Smeared-charge approaches were addressed to consider atomic charge distributions instead of point-charges.[91−95] In this work, a Gaussian distribution $\rho_I(r_i)$ is used for each atom[87,88]

$$\rho_I(r_i) = q_I \left(\frac{\Phi_I^*}{\pi}\right)^{3/2} e^{-\Phi_I^* r_i^2} \tag{9}$$

dx.doi.org/10.1021/jp507639z | J. Phys. Chem. A 2014, 118, 11282−11292

in which r_i is an electronic coordinate and the width of the Gaussian distribution, Φ_I^*, is an additional atom-type parameter of the model. The distribution is normalized to give the atomic charge q_I. The interaction between two Gaussian charge distributions may be written as[88]

$$\tilde{V} = q_I \tilde{T}_{IJ}^{(0)} q_J = \frac{q_I q_J}{\tilde{R}_{IJ}} \tag{10}$$

where $\tilde{R}_{IJ}$ is a modified distance, $\tilde{T}_{IJ}^{(0)} = 1/\tilde{R}_{IJ}$, given by the regular error function $\tilde{R}_{IJ} = R_{IJ}/\mathrm{erf}((a_{IJ})^{1/2}R_{IJ})$, and a_{IJ} is

$$a_{IJ} = \frac{\Phi_I^* \Phi_J^*}{\Phi_I^* + \Phi_J^*} \tag{11}$$

While the error function has been employed in charge−dipole models,[78−82] an approximation of this function is considered in our work[88,96]

$$\tilde{R}_{IJ} = \sqrt{{R_{IJ}}^2 + \frac{\pi}{4a_{IJ}}} \tag{12}$$

which has the same limiting behavior at $R_{IJ} \to 0$ and $R_{IJ} \to \infty$ as $\tilde{R}_{IJ} = R_{IJ}/\mathrm{erf}((a_{IJ})^{1/2}R_{IJ})$. While the charge−dipole interaction tensor, $\tilde{T}_{IJ,\alpha}^{(1)}$, and the dipole−dipole interaction tensor, $\tilde{T}_{IJ,\alpha\beta}^{(2)}$, have been approximated as the first and second derivatives of $\tilde{T}_{IJ}^{(0)}$ with respect to $\tilde{R}_{IJ}$,[88] $\tilde{T}_{IJ,\alpha}^{(1)}$ and $\tilde{T}_{IJ,\alpha\beta}^{(2)}$ are in this work obtained by the derivatives of $\tilde{T}_{IJ}^{(0)}$ with respect to R_{IJ} as discussed in our recent work[36]

$$\tilde{T}_{IJ,\alpha}^{(1)} = \frac{\partial \tilde{T}_{IJ}^{(0)}}{\partial R_{IJ,\alpha}} = -\frac{R_{IJ,\alpha}}{{\tilde{R}_{IJ}}^3} \quad \text{and}$$
$$\tilde{T}_{IJ,\alpha\beta}^{(2)} = \frac{\partial \tilde{T}_{IJ,\alpha}^{(1)}}{\partial R_{IJ,\beta}} = \frac{3R_{IJ,\alpha}R_{IJ,\beta}}{{\tilde{R}_{IJ}}^5} - \frac{\delta_{\alpha\beta}}{{\tilde{R}_{IJ}}^3} \tag{13}$$

in which $\delta_{\alpha\beta}$ is the Kronecker delta function, the subscripts, α and β, denote one of the Cartesian coordinates, x, y or z, and the Einstein summation convention is used for repeated subscripts. $\tilde{T}_{IJ,\alpha}^{(1)} \to 0$ when $R_{IJ} \to 0$, however, the $\tilde{T}_{IJ,\alpha\beta}^{(2)}$ tensor in eq 13 is not traceless, and for including quadrupole moments in the model normally a traceless formalism should be considered.[97]

For the polarizability to scale properly with the size of the system both for metallic and nonmetallic systems, we make two approximations to eq 8. First, eq 8 is in the three-particle case given as

$$\tilde{T}_{IK,IM}^{(0)} = \eta_I^* - \tilde{T}_{KI}^{(0)} - \tilde{T}_{IM}^{(0)} + \tilde{T}_{KM}^{(0)}, \quad I = J \text{ and } K \neq M \tag{14}$$

where the chemical hardness, η_I^* is modified as[37]

$$\eta_I^* \to \eta_I^* S_{IK}^{-1/2} S_{IM}^{-1/2} g_{I,KM}, \quad I = J \text{ and } K \neq M \tag{15}$$

where $g_{I,KM}$ is a function of the two distances, R_{IK} and R_{IM}, describing a resistance for charge flow in the molecule, modeled as[36]

$$g_{I,KM} = (g_{0,I}^*)^2 g_{0,K}^* g_{0,M}^* H_{I,KM}(\Delta_{I,KM}) + (g_{1,I}^*)^2 g_{1,K}^* g_{1,M}^* (1 - H_{I,KM}(\Delta_{I,KM})) \tag{16}$$

where $g_{0,I}^*$ and $g_{1,I}^*$ are atom-type parameters and $H_{I,KM}$ is a smooth step function

$$H_{I,KM}(\Delta) = \frac{1}{2}(1 + \tanh(C_{I,KM}\Delta_{I,KM})) \tag{17}$$

in which $C_{I,KM} = (C_I^*)^2 C_K^* C_M^*$ and $\Delta_{I,KM} = R_{IK} - (R_I^* + R_K^*) + R_{IM} - (R_I^* + R_M^*)$ where C_I^* and R_I^* are atom-type parameters. In eq 15, S_{IK} is

$$S_{IK} = \mathrm{e}^{-a_{IK}(R_{IK} - R_I^* - R_K^*)^2} \tag{18}$$

where a_{IK} is given in eq 11.

Second, we modify eq 8 for a large separation between two particles, by regarding $K = M$ and $I = J$. In this case, $\tilde{T}_{IK,JM}^{(0)}$ becomes $\eta_I^* + \eta_K^* - 2\tilde{T}_{IK}^{(0)}$ and the modification of the chemical hardness in $\tilde{T}_{IK,IK}^{(0)}$ is introduced as[37]

$$(\eta_I^* + \eta_K^*) \to (\eta_I^* + \eta_K^*) {S_{IK}}^{-1} \tag{19}$$

If $g_{I,KK} = 1$, eq 19 is a special case of eq 15. Equation 19 solves the two-particle problem, i.e., it penalizes the charge-transfer between two particles at infinite separation, whereas eq 15 addresses the "long-chain" problem, i.e., an energy cost is added for charge transport in an extended system.

The charge-dipole interaction energy $V^{q\mu}$ is rewritten in terms of charge-transfer variables as[37]

$$V^{q\mu} = \sum_{I,J}^{N} q_I \tilde{T}_{IJ,\alpha}^{(1)} \mu_{J,\alpha} = \sum_{I,K>I,J}^{N} q_{IK} \tilde{T}_{IK,J,\alpha}^{(1)} \mu_{J,\alpha} \tag{20}$$

where $\tilde{T}_{IK,J,\alpha}^{(1)} = \tilde{T}_{IJ,\alpha}^{(1)} - \tilde{T}_{KJ,\alpha}^{(1)}$.

The dipole−dipole interaction energy $V^{\mu\mu}$ in the point-dipole interaction (PDI) model is expressed by[37]

$$V^{\mu\mu} = \frac{1}{2}\sum_{I}^{N} \mu_{I,\alpha}(\alpha_{I,\beta\alpha})^{-1}\mu_{I,\beta} - \frac{1}{2}\sum_{I}^{N}\sum_{K\neq I}^{N} \mu_{I,\alpha}\tilde{T}_{IK,\alpha\beta}^{(2)}\mu_{K,\beta} - \sum_{I}^{N} E_{I,\alpha}^{\mathrm{ext}}\mu_{I,\alpha} \tag{21}$$

where $\alpha_{I,\beta\alpha}$ is the atomic polarizability and $E_{I,\alpha}^{\mathrm{ext}}$ is the external electric field at atom I. Also, $\alpha_{I,\beta\alpha}$ is modified to include the chemical surroundings[36,92]

$$\alpha_{I,\beta\alpha} = \alpha_I^*(\delta_{\beta\alpha} + x_I^*(1 - G_{I,\beta\alpha})) \tag{22}$$

where α_I^* and x_I^* are atom-type parameters which introduce the isotropy and the anisotropy of the atomic polarizability, respectively, and $G_{I,\beta\alpha}$ reads

$$G_{I,\beta\alpha} = \frac{3}{\mathrm{Tr}(\Gamma_I)}\Gamma_{I,\beta\alpha} \tag{23}$$

in which $\Gamma_{I,\beta\alpha}$ is expressed by

$$\Gamma_{I,\beta\alpha} = \sum_{J\neq I}^{N} \alpha_J^* S_{IJ} \frac{R_{IJ,\beta}R_{IJ,\alpha}}{{R_{IJ}}^2} \tag{24}$$

Here, $R_{IJ,\beta}R_{IJ,\alpha}/R_{IJ}^2$ results in the correct rotational properties of $\alpha_{I,\beta\alpha}$ and S_{IJ} is given by eq 18.

The charge-transfer terms and the atomic dipole moments are assumed to oscillate with the same frequency, ω, as the external electric field, $E_{J,\alpha}^{\mathrm{ext}} = \mathrm{Re}(E_{J,\alpha}^{(\omega)}\mathrm{e}^{i\omega t})$, and electrostatic potential, $\varphi_{IJ}^{\mathrm{ext}} = \mathrm{Re}(\varphi_{I,J}^{(\omega)}\mathrm{e}^{i\omega t})$, so that $q_{IK} = \mathrm{Re}(q_{IK}^{(0)} + q_{IK}^{(\omega)}\mathrm{e}^{i\omega t})$ and $\mu_{I,\alpha} = \mathrm{Re}(\mu_{I,\alpha}^{(0)} + \mu_{I,\alpha}^{(\omega)}\mathrm{e}^{i\omega t})$, respectively. In matrix form, the linear response equations, including nonzero dissipation in the frequency-dependence, are written as[36]

dx.doi.org/10.1021/jp507639z | J. Phys. Chem. A 2014, 118, 11282−11292

Table 1. Molecules Included in the Study

molecules in the training set	molecules in the validation set
azobenzene	2-methylazobenzene
benzene	4,4′-dimethylazobenzene
4-methylazobenzene	4-amino-4′-methylazobenzene
3-methylazobenzene	4-diethylaminoazobenzene
4-aminoazobenzene	4,4′-di(dimethylamino)azobenzene
4,4′-diaminoazobenzene	4-cyano-4′-dimethylaminoazobenzene
4-dimethylaminoazobenzene	4-cyano-4′-diethylaminoazobenzene
4-methyl-4′-dimethylaminoazobenzene	2,4,6-tricyano-4′-diethylaminoazobenzene
4,4′-di(diethylamino)azobenzene	
4-cyanoazobenzene	

Table 2. Atom-Type Parameters Obtained for the Model (a.u.)

	η^*	α^*	x^*	Φ^*	g_0^*	g_1^*	C^*	R^*	c^{q*}	$c^{\mu*}$	γ^{q*}	$\gamma^{\mu*}$
H	2.0820	3.9515	0.4875	0.4628	0.3241	0.0749	1.2765	0.7619	6.1514	0.6823	0.0069	0.0106
C	4.3183	8.2597	0.1994	1.2011	0.6010	0.9411	0.6644	1.5895	1.0270	0.9713	0.0076	0.0147
N	3.0987	5.9671	0.1846	1.7134	1.0934	1.2051	14.6102	1.1603	2.2770	2.6491	0.0173	0.0060
H[36]	0.2300	1.6500	0.3200	1.0200	1.0000				0.0300	0.6300		
C[36]	1.0300	8.3500	0.3800	0.4300	0.7700	0.9957	4.1300	1.4100	0.6100	0.5900		

$$\left\{\begin{pmatrix} \tilde{T}^{(0)} & \tilde{T}^{(1)} \\ (\tilde{T}^{(1)})^t & -\tilde{T}^{(2)} \end{pmatrix} - \omega^2 \begin{pmatrix} C^q & 0 \\ 0 & C^\mu \end{pmatrix}\right\}\begin{pmatrix} q \\ \mu \end{pmatrix} = \begin{pmatrix} -\varphi \\ E \end{pmatrix} \tag{25}$$

where $\tilde{T}^{(0)}$, $\tilde{T}^{(1)}$ and $\tilde{T}^{(2)}$ are $M \times M$, $M \times 3N$, and $3N \times 3N$ matrices where one element of them is defined by $\tilde{T}^{(0)}_{SP,JM}$, $\tilde{T}^{(1)}_{SP,K,\beta}$ and $\tilde{T}^{(2)}_{IK,\alpha\beta}$, $\tilde{T}^{(2)}_{II,\alpha\beta} = (\alpha_{I,\beta\alpha})^{-1}$, respectively. The frequency-dependent contribution is found by subtracting a diagonal matrix in eq 25.[38] C^q is an $M \times M$ diagonal matrix in which one element reads $(c_J^{q*} + c_M^{q*})R_{JM}{}^2(1-(i/2\omega)(\gamma_J^{q*} + \gamma_M^{q*}))\delta_{SJ}\delta_{PM}$ while C^μ is a $3N \times 3N$ diagonal matrix and one element of the matrix is given by $c_K^{\mu*}(1 - i\gamma_K^{\mu*}/\omega)\delta_{IK}\delta_{\alpha\beta}$ where the c_J^{q*} parameter appears in the kinetic energy in eq 3 whereas $c_K^{\mu*}$ appears in the kinetic energy in eq 4. The charge and dipole dissipation are taken into account by exchanging ω^2 with $\omega^2 - i(1/2)(\gamma_I^{q*} + \gamma_K^{q*})\omega$ and $\omega^2 - i\gamma_I^{\mu*}\omega$ in the diagonal matrix in which γ_J^{q*} and $\gamma_K^{\mu*}$ are dissipation parameters for charges and dipoles, respectively.[38] Hence, q and μ are $M \times 1$ and $3N \times 1$ matrices with the elements given by $q_{JM}^{(\omega)}$ and $\mu_{K,\beta}^{(\omega)}$, respectively. Likewise, on the right-hand side of eq 25, φ is an $M \times 1$ matrix with the elements $\varphi_{SP}^{(\omega)}$ and E is a $3N \times 1$ matrix where one element of this matrix is expressed by $E_{I,\alpha}^{(\omega)}$. We note that M and N are the number of bonds and atoms, respectively.

For a homogeneous electric field, the applied perturbation reduces to $E_{I,\alpha}^{(\omega)} = E_\alpha^{(\omega)}$ and $\varphi_{SP}^{(\omega)} = -(R_{S,\alpha} - R_{P,\alpha})E_\alpha^{(\omega)}$, respectively. The molecular polarizability $\alpha_{\alpha\beta}(\omega)$ is thus obtained from the derivative of eq 25 with respect to a homogeneous external electric field which is the actual linear set of equations solved in the model and is obtained as[36]

$$\alpha_{\alpha\beta}(\omega) = \frac{\partial \mu_\alpha^{(\omega)}}{\partial E_\beta^{(\omega)}} = \sum_{I,M>I}^{N} R_{IM,\alpha}\frac{\partial q_{IM}^{(\omega)}}{\partial E_\beta^{(\omega)}} + \sum_{I}^{N}\frac{\partial \mu_{I,\alpha}^{(\omega)}}{\partial E_\beta^{(\omega)}}$$

To obtain the polarizability tensor, the model has to be solved three times, for $\beta = x, y, z$.

III. CALCULATIONS AND PARAMETRIZATION

In this work, TDDFT is used to obtain the reference data for the parametrization of the model for a set of azobenzene compounds. The full complex polarizability tensor has been calculated and is included in the parametrization for the molecules listed in Table 1 although only isotropic polarizabilities are presented. The ADF software is used for the DFT computations.[98−100] The PBE[101] functional has been adopted. For the polarizability calculations, the ATZP[102,103] basis set is used and for the geometry optimizations, the TZP[102] basis set is employed, respectively. A value of $\gamma = 0.004$ hartree is used for the lifetime parameter, γ, in the calculations of the frequency-dependent polarizabilites.[104]

A group of ten molecules is chosen as a training set (see the left side of Table 1), where the molecules contain the elements carbon, hydrogen, and nitrogen. A genetic algorithm is employed in the first parametrization step for obtaining reasonable values for the parameters, but they are regarded only as a good starting point for the parametrization. Next, a simplex algorithm is utilized to find a better set of parameters. The number of molecules to parametrize the model are gradually increased. The optimum parameters were obtained by minimizing the relative root-mean square deviation of the frequency-dependent polarizability tensor between the CT/PDI and the DFT calculations. After performing parametrization on the training set, the model is validated for the molecules on the right side of Table 1.

The atom-type parameters used in this work are the isotropic and anisotropic atomic polarizability parameters α^* and x^*, respectively, given in eq 22, the chemical hardness η^* presented in eq 15, a width of a Gaussian charge distribution Φ^*, which describes the damping of electrostatics and the overlap between charge distributions in eq 18. To model the nonmetallic behavior of the charge-transfer within a molecule, a three-atom resistance term, $g_{I,KM}$ is adopted including four atom-type parameters g_0^*, g_1^*, C^*, and R^*, given by eq 16.[36] Finally, four parameters are used to model the frequency-dependence. c^{q*} and $c^{\mu*}$ are interpreted as the inverse of the number of oscillating charges and included in the charge and the dipole kinetic energies in eqs 3 and 4, respectively, whereas γ^{q*} and $\gamma^{\mu*}$ describe the charge and dipole dissipation, respectively.

The parameters obtained here and in our previous work[36] for C and H are given in Table 2. There are several notable differences between the carbon and hydrogen parameters

dx.doi.org/10.1021/jp507639z | J. Phys. Chem. A 2014, 118, 11282−11292

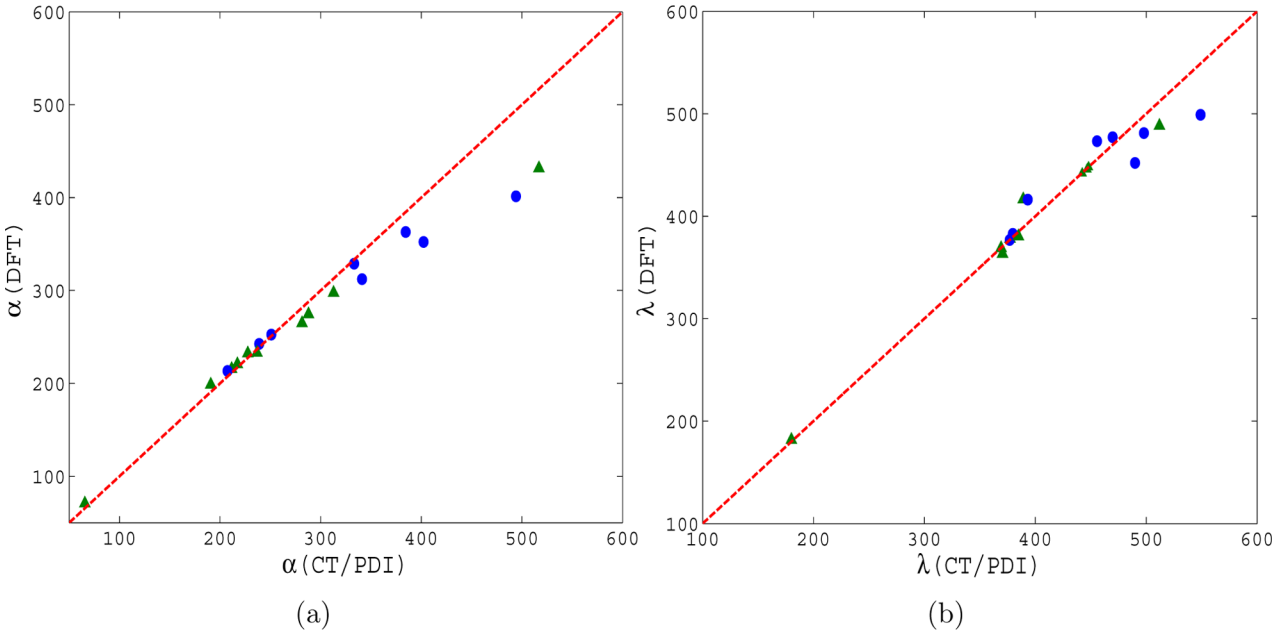

Figure 1. (a) Static polarizability of the azo compounds, DFT vs CT/PDI model. (b) Excitation wavelength of the azo compounds, DFT vs CT/PDI model. The points shown by triangles are compounds in the training set while the circles represent molecules in the validation set. The dashed lines are a help for the eye to show a perfect parametrization.

obtained in the two parametrizations. First, the Φ_C^* parameter has increased from 0.43 to 1.2, which corresponds to a narrower charge distribution. The opposite occurs for the Φ_H^* parameter decreasing from 1.02 to 0.46, giving the hydrogen atoms a broader charge distribution. The Φ^* parameters have in our previous work[36,37,62,63,88] always been sensitive to details in the model and for an atom pair, e.g., C and H, the parameter values can be shifted between the two atom types without modifying a_{IJ} in eq 11. Second, the η^* parameters for both carbon and hydrogen have been assigned significantly higher values here, rendering charge-transfer more expensive. For hydrogen, the atomic polarizability α_H^* increases from 1.65 to 3.95 a.u. while the anisotropy parameter for the polarizability, x_H^* has increased from 0.32 to 0.48. However, also these two parameters are strongly coupled, and the effect by the new parameters is that the hydrogens are more polarizable in the direction of its chemical bond and almost not polarizable at all in the other directions. This is reasonable since the electron of the hydrogen is involved in a σ-bond. Also note that the x_I^* parameter has to be in the range 0−0.5, where 0 gives an isotropic polarizability and 0.5 gives the highest possible anisotropy. In addition, the c_H^{q*} parameter increases by a factor of 200, indicating that the parameter now has a larger weight in the parametrization. There are significant changes in the carbon and hydrogen parameters as compared to our previous calibration,[36] but it seems to be a common problem in fluctuating charge models.[105]

For the nitrogen parameters, two features are noted. First, the $c_N^{\mu*}$ parameter is approximately three times higher than both $c_C^{\mu*}$ and $c_H^{\mu*}$. Therefore, there are less electronic charge participating in the point-dipole oscillations for nitrogen than for the other two elements. Second, the polarizability, α_N^*, has as expected a value in between that of hydrogen and carbon, in agreement with the experimental and theoretical investigations.[106] Generally speaking, the actual values of the parameters are not well established. Still the long-term goal is to establish a single set of atom-type parameters able to describe all systems, and if needed we will improve the physics of the model rather than providing different parameters for different types of molecular systems.

To demonstrate the accuracy of our parametrization, we compare the result of our model with DFT in Figure 1 for the static polarizability and the excitation wavelengths of the azo compounds listed in Table 1, which shows in general a good agreement. The static polarizability of 4,4′-di(dimethylamino)-azobenzene, 4,4′-di(diethylamino)azobenzene, and 2,4,6-tricyano-4′-diethylaminoazobenzene show the largest deviations from the reference values, while the largest errors for the excitation wavelengths appear in 4-aminoazobenzene, 4-diethylaminoazobenzene, and 2,4,6-tricyano-4′-diethylaminoazobenzene.

IV. RESULTS AND DISCUSSION

Figure 2 shows the isotropic polarizability for eight representative molecules given in Table 1. The figure is constructed of eight panels: (a) benzene, (b) azobenzene, (c) 4-aminoazobenzene, (d) 4-cyanoazobenzene, (e) 4,4′-dimethylazobenzene, (f) 4-diethylaminoazobenzene, (g) 4,4′-di(dimethylamino)azobenzene, and (h) 4-cyano-4′-diethylaminoazobenzene where four of them are in the training set, (a)−(d), whereas the other four are in the validation set, (e)−(h). Because of different excitation energies between benzene and the azo compounds, different scales are used in panel (a) as compared to the other panels.

As seen in Figure 2(a) and (b) for the benzene and azobenzene molecules, the CT/PDI model and the DFT reference data are in good agreement for both the static polarizability and the position of the absorption peaks. It is crucial for the model to be able to model adequately the difference in excitation energy between an azo bond and an aromatic ring, which is the reason for that the benzene molecule is included in the training set.

In this work, we investigate three different types of substituents in the azo compounds: alkyl, amino, and cyano

dx.doi.org/10.1021/jp507639z | J. Phys. Chem. A 2014, 118, 11282−11292

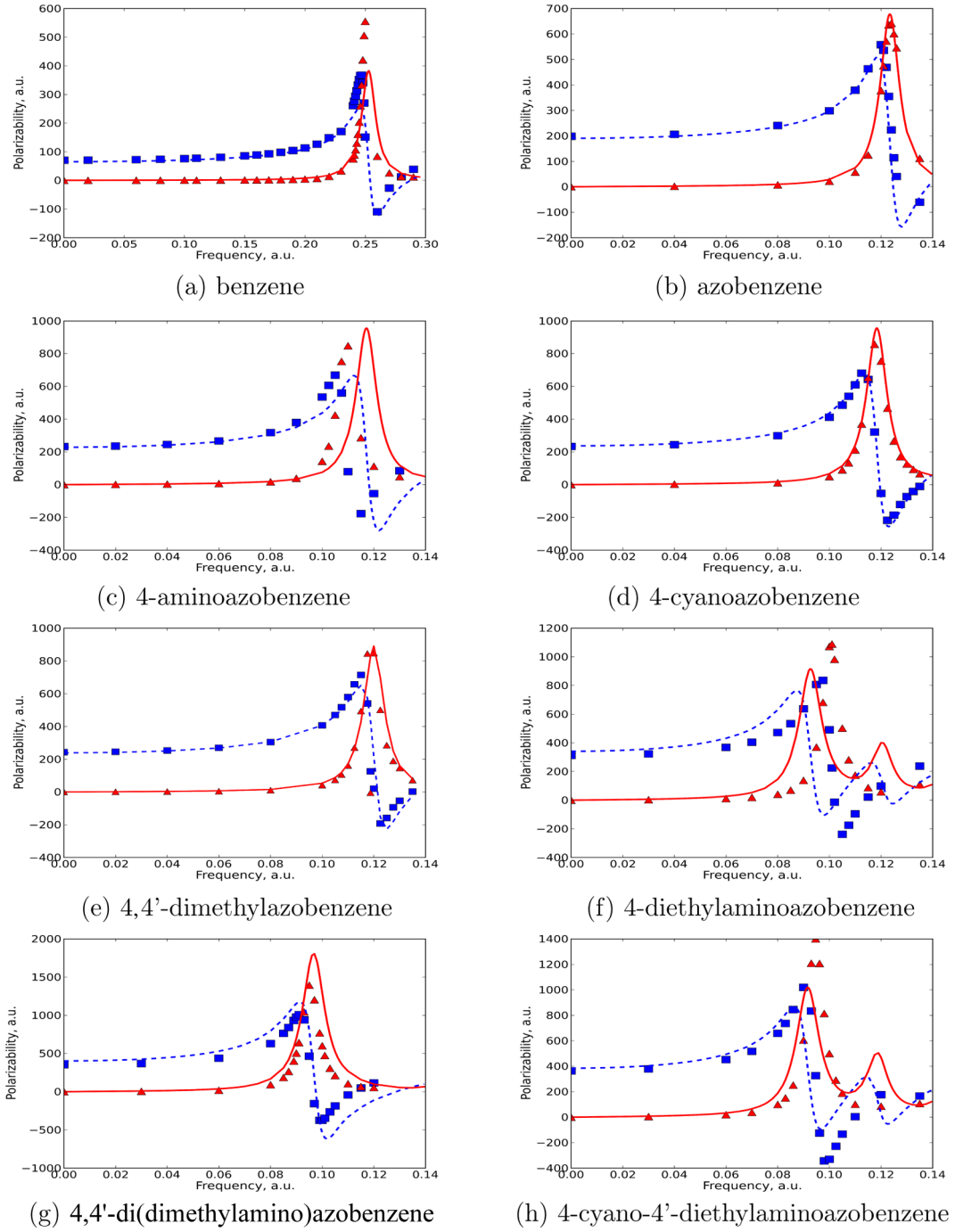

Figure 2. Polarizability. The solid and dashed curves represent the CT/PDI model while the triangles and squares show the DFT calculations. The blue features correspond to the real parts of polarizability whereas the red features correspond to the imaginary part.

groups. Alkyl groups are generally known as electron-donors compared to hydrogen,[107] whereas cyano groups are known as moderate electron-accepting substituents by resonance effects. In between, the amino groups are expected to have both electron-donating and accepting characteristics due to the resonance donation of π-electron to the ring and an inductive acceptance of electrons from the ring, respectively.[108] By replacing hydrogen atoms in the azobenzene molecule with electron-donating and/or electron-accepting substituents, electron-donating substituents shift the excitation energy by effectively raising the energy level of the π-orbital, while electron-accepting substituents shift the excitation energy by effectively lowering the level of the π^*-orbital.[109] Figure 2(e) shows 4,4′-dimethylazobenzene, Figure 2(d) and (h) shows cyano substituents, 4-cyanoazobenzene and 4-cyano-4′-diethylaminoazobenzene, respectively, whereas the remaining panels in Figure 2 display representative molecules with amino substituents. As seen in Figure 2, the excitation energies are reduced by the substitutions demonstrating that the CT/PDI model is in good agreement with the DFT calculations. Considering Figure 2(e)−(h), the static polarizability and excitation energies are in good agreement with the reference data although they were not included in the training set. Hence,

dx.doi.org/10.1021/jp507639z | J. Phys. Chem. A 2014, 118, 11282−11292

Table 3. Results and Comparisons: Static Polarizability and Excitation Wavelength

		static polarizability (a.u.)			$\pi \rightarrow \pi^*$ wavelength (nm)			
	molecules	CT/PDI	DFT	error %	CT/PDI	DFT	error %	exptl
training set	benzene	65.55	70.9	7.54	180.0	181.82	0.95	253[111]
	azobenzene	190.70	198.7	4.02	369.24	368.94	0.08	318[112]
	4-methylazobenzene	217.28	220.8	1.59	377.18	378.12	0.24	333[112]
	3-methylazobenzene	211.52	215.5	1.84	370.44	363.35	1.91	322[22]
	4-aminoazobenzene	227.62	232.4	2.05	389.10	416.49	7.03	389[89]
	4,4′-diaminoazobenzene	281.48	264.9	6.25	442.37	441.94	0.09	
	4-dimethylaminoazobenzene	287.91	274.5	4.88	446.71	445.83	0.19	407[113]
	4-methyl-4′-dimethylaminoazobenzene	312.86	297.6	5.12	448.02	448.02	0.00	407[113]
	4,4′-di(diethylamino)azobenzene	516.86	432.6	19.48	511.95	488.36	4.60	426[114]
	4-cyanoazobenzene	236.71	233.0	1.59	384.83	380.33	1.16	325[22]
validation set	2-methylazobenzene	207.43	213.4	2.79	376.87	376.87	0.00	
	4,4′-dimethylazobenzene	238.92	242.5	1.50	379.70	382.89	0.84	
	4-amino-4′-methylazobenzene	250.94	252.5	0.61	393.13	416.11	5.84	
	4-diethylaminoazobenzene	341.16	312.6	9.14	489.93	452.02	7.73	415[112]
	4,4′-di(dimethylamino)azobenzene	402.34	353.3	13.90	469.73	477.11	1.57	421[115]
	4-cyano-4′-dimethylaminoazobenzene	333.28	328.9	1.32	455.64	473.15	3.84	451[116]
	4-cyano-4′-diethylaminoazobenzene	384.43	363.0	5.90	497.97	481.14	3.37	466[117]
	2,4,6-tricyano-4′-diethylaminoazobenzene	494.17	401.4	23.11	548.96	499.06	9.09	562[117]

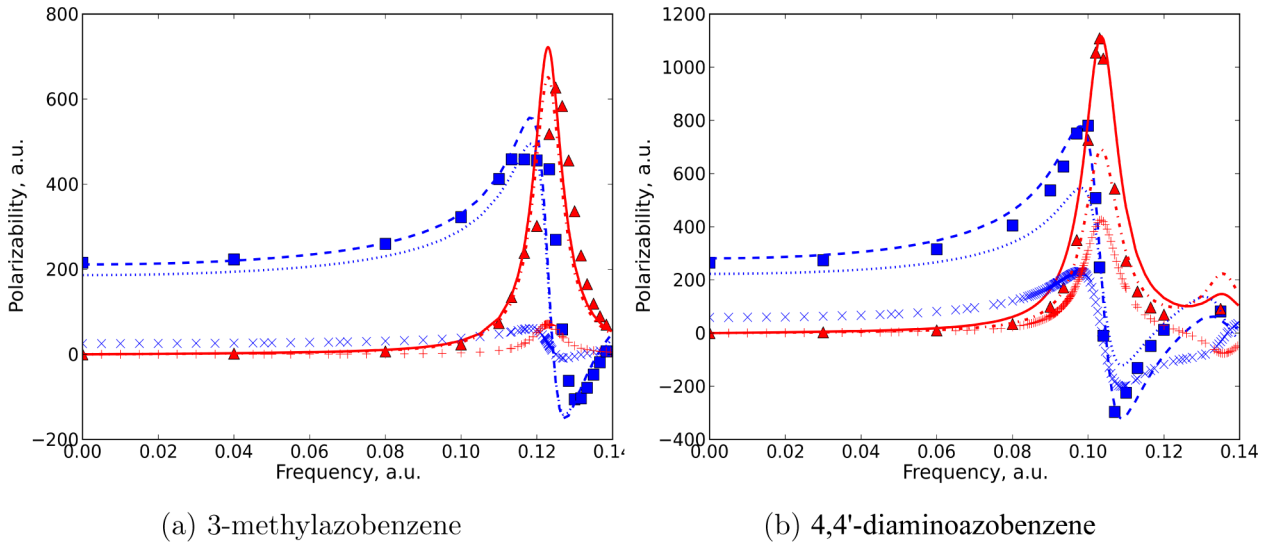

Figure 3. Isotropic polarizability. The solid and dashed curves represent the CT/PDI model while the triangles and squares show the DFT reference data. Crosses (×) and pluses (+) exhibit charge-transfer contributions whereas dotted and dash-dotted curves show the contributions of dipole moments. The blue features correspond to the real parts, while the red features correspond to imaginary parts of the polarizability.

the results illustrate a transferability of the atom-type parameters for the molecules within the validation set.

Table 3 presents the static polarizability and the $\pi \rightarrow \pi^*$ excitation wavelengths for all molecules in Table 1. The largest errors of our model are around 23% for the static polarizability and 9% for the $\pi \rightarrow \pi^*$ excitation wavelengths as compared to the DFT calculations. The largest errors appear in 2,4,6-tricyano-4′-diethylaminoazobenzene molecule with four substituents including three cyano groups and one alkyl-amino substituent. As seen in Table 3, the static polarizability increases by adding substituents to azobenzene, in line with results for additive models for the molecular polarizability.[110] 4,4′-di(diethylamino)azobenzene has the largest static polarizability and a large $\pi \rightarrow \pi^*$ excitation wavelength in both the CT/PDI model and in the DFT calculations, which is attributed to substantial charge-transfer and point-dipole moment contributions in the two alkyl-amino substituents. The experimental data for the $\pi \rightarrow \pi^*$ excitation wavelengths given in Table 3 show the same trend as our model and DFT results, although there is a shift compared to experimental data. In the CT/PDI model and in the DFT calculations, we consider molecules in the gas phase while the measured experimental data are in an ethanol solvent. The DFT calculations show a lower excitation wavelength for 3-methylazobenzene as compared to azobenzene, whereas the CT/PDI model shows an increasing wavelength compared to azobenzene in agreement with experiments.

In Figure 3, the isotropic polarizability as well as its charge-transfer and point-dipole moment contributions are presented for two typical molecules, (a) 3-methylazobenzene and (b) 4,4′-diaminoazobenzene. In Figure 3(a), the point-dipole term dominates as compared to the charge-transfer portion whereas

dx.doi.org/10.1021/jp507639z | J. Phys. Chem. A 2014, 118, 11282−11292

in Figure 3(b) the charge-transfer portion is more significant. For all molecules in Table 1, the point-dipole contributions mainly determine the frequency-dependent polarizability. Close to absorption, the point-dipole contributions arise mainly from the nitrogen atoms in the azo bond and the adjacent carbon atoms in particular for the azo compounds possessing alkyl, amino, and cyano groups. In the molecules with alkyl-amino substituents, however, the nitrogen atoms of the alkyl-amino groups have the largest point-dipole contributions to the polarizability at the absorption frequency. We also note that all substituents enhance the contribution of the charge-transfer contribution to the polarizability especially alkyl-amino substituents, and that a charge-transfer effect is introduced by the substituents on the phenyl rings giving a shift in the $\pi \rightarrow \pi^*$ excitation energy. The shift of the $\pi \rightarrow \pi^*$ excitation energy found in this work by substituents is in agreement with previous work on azo compounds.[10,11,21,22,89,90]

V. CONCLUSIONS

We have studied the frequency-dependent polarizability and the $\pi \rightarrow \pi^*$ excitation energy of azo compounds using the CT/PDI model. The point-dipole contribution dominates over the charge-transfer term for the molecules included in this study. Close to absorption, the point-dipole contributions of the nitrogen atoms in the azo bond and the adjacent carbon atoms give the main contribution for the frequency-dependent polarizability. Also, our calculations reveal a charge-transfer contribution to the total polarizability due to substituents, where the charge-transfer contributions introduce a shift in the $\pi \rightarrow \pi^*$ excitation energy consistent with DFT and experiments. Therefore, it is concluded that the presented model is capable of modeling the frequency-dependent polarizability through the $\pi \rightarrow \pi^*$ excitation energy for a set of molecules that we have assumed to be challenging since the excitation wavelength is strongly affected by substituents relatively far away from the excitation which is essentially localized to the azo bond.

Finally, many atomistic polarization models in the literature consist of either a charge term or a point polarizability term. These two terms have a different physical behavior and can not be replaced by each other, and in this work the coupling between the two terms is found to be crucial to model excitation energies.

AUTHOR INFORMATION

Corresponding Author

*E-mail: per-olof.aastrand@ntnu.no.

Notes

The authors declare no competing financial interest.

ACKNOWLEDGMENTS

A grant of computer time is acknowledged from the NOTUR project (account 2920k) at the Norwegian Research Council. N.D. and P.-O.Å. acknowledge a research grant (200631/560) funded by the Norwegian Research Council, ABB, and Statnett.

REFERENCES

(1) Griffiths, J. II. Photochemistry of Azobenzene and its Derivatives. *Chem. Soc. Rev.* **1972**, *1*, 481−493.
(2) Griffiths, J. *Colour and Constitution of Organic Molecules*; Academic Press: New York, 1976.
(3) Venkataraman, K. *The chemistry of synthetic dyes*; Academic Press: New York, 1956.
(4) Christie, R. M. *Colour Chemistry*; Royal Society of Chemistry: Cambridge, 2001.
(5) Eich, M.; Wendorff, J. H.; Reck, B.; Ringsdorf, H. Reversible Digital and Holographic Optical Storage in Polymeric Liquid Crystals. *Makromol. Chem. Rapid Commun.* **1987**, *8*, 59−63.
(6) Wiesner, U.; Antonietti, M.; Boeffel, C.; Spiess, H. W. Dynamics of Photoinduced Isomerization of Azobenzene Moieties in Liquid-Crystalline Polymers. *Makromol. Chem.* **1990**, *191*, 2133−2149.
(7) Natansohn, A.; Rochon, P.; Gosselin, J.; Xie, S. Azo Polymers for Reversible Optical Storage. 1. Poly[4-[[2-(Acryloyloxy)Ethyl]-Ethylamino]-4-Nitroazobenzene]. *Macromolecules* **1992**, *25*, 2268−2273.
(8) Hvilsted, S.; Andruzzi, F.; Ramanujam, P. S. Side-Chain Liquid-Crystalline Polyesters for Optical Information Storage. *Opt. Lett.* **1992**, *17*, 1234−1236.
(9) Berg, R. H.; Hvilsted, S.; Ramanujam, P. S. Peptide Oligomers for Holographic Data Storage. *Nature* **1996**, *383*, 505−508.
(10) Åstrand, P.-O.; Larsen, P. S.; Hvilsted, S.; Ramanujam, P. S.; Bak, K. L.; Sauer, S. P. A. Five-Membered Rings as Diazo Components in Optical Data Storage Devices: an Ab Initio Investigation of the Lowest Singlet Excitation Energies. *Chem. Phys. Lett.* **2000**, *325*, 115−119.
(11) Åstrand, P.-O.; Ramanujam, P. S.; Hvilsted, S.; Bak, K. L.; Sauer, S. P. A. Ab Initio Calculation of the Electronic Spectrum of Azobenzene Dyes and its Impact on the Design of Optical Data Storage Materials. *J. Am. Chem. Soc.* **2000**, *122*, 3482−3487.
(12) Beharry, A. A.; Woolley, G. A. Azobenzene Photoswitches for Biomolecules. *Chem. Soc. Rev.* **2011**, *40*, 4422−4437.
(13) Bandara, H. M. D.; Burdette, S. C. Photoisomerization in Different Classes of Azobenzene. *Chem. Soc. Rev.* **2012**, *41*, 1809−1825.
(14) Yan, D.; Lu, J.; Wei, M.; Evans, D. G.; Duan, X. Recent Advances in Photofunctional Guest/Layered Double Hydroxide Host Composite Systems and Their Applications: Experimental and Theoretical Perspectives. *J. Mater. Chem.* **2011**, *21*, 13128−13139.
(15) Ishikawa, T.; Noro, T.; Shoda, T. Theoretical Study on the Photoisomerization of Azobenzene. *J. Chem. Phys.* **2001**, *115*, 7503−7512.
(16) Cembran, A.; Bernardi, F.; Garavelli, M.; Gagliardi, L.; Orlandi, G. On the Mechanism of the cis-trans Isomerization in the Lowest Electronic States of Azobenzene: S_0, S_1, and T_1. *J. Am. Chem. Soc.* **2004**, *126*, 3234−3243.
(17) Crecca, C. R.; Roitberg, A. E. Theoretical Study of the Isomerization Mechanism of Azobenzene and Disubstituted Azobenzene Derivatives. *J. Phys. Chem. A* **2006**, *110*, 8188−8203.
(18) Rau, H. *Photochromism: Molecules and Systems*; Durr, H., Bouas-Laurent, H., Ed.; Elsevier: Amsterdam, 1990.
(19) *Molecular Switches*; Feringa, B. L., Ed.; Wiley-VCH: Weinheim, Germany, 2001.
(20) Dubecký, M.; Derian, R.; Horváthová, L.; Allan, M.; Stich, I. Disentanglement of Triplet and Singlet States of Azobenzene: Direct EELS Detection and QMC Modeling. *Phys. Chem. Chem. Phys.* **2011**, *13*, 20939−20945.
(21) Mustroph, H.; Epperlein, J. Quantitative Beschreibung der Absorptionsmaxima Mehrfach Substituirter Azobenzene mit Einem Inkrementsystem. *J. Prakt. Chem.* **1981**, *323*, 755−775.
(22) Jaffé, H. H.; Yeh, S. J.; Gardner, R. W. The Electronic Spectra of Azobenzene Derivatives and Their Conjugate Acids. *J. Mol. Spectrosc.* **1958**, *2*, 120−136.
(23) Dickey, J. B.; Towne, E. B.; Bloom, M. S.; Moore, W. H.; Hill, H. M.; Heynemann, H.; Hedberg, D. G.; Sievers, D. C.; Otis, M. V. Azo Dyes from Substituted 2-Aminothiazoles. *J. Org. Chem.* **1959**, *24*, 187−196.
(24) Towns, A. D. Development in Azo Disperse Dyes Derived from Heterocyclic Diazo Compounds. *Dyes Pigm.* **1999**, *42*, 3−28.
(25) Kanis, D. R.; Ratner, M. A.; Marks, T. J. Design and Construction of Molecular Assemblies with Large Second-Order Optical Nonlinearities. Quantum Chemical Aspects. *Chem. Rev.* **1994**, *94*, 195−242.

(26) Prasad, P. N.; Williams, D. J. *Introduction to Nonlinear Optical Effects in Molecules and Polymers*; Wiley: New York, 1991.
(27) Runge, E.; Gross, E. K. U. Density-Functional Theory for Time-Dependent Systems. *Phys. Rev. Lett.* **1984**, *52*, 997−1000.
(28) Gross, E. K. U.; Dobson, J. F.; Petersilka, M. Density Functional Theory of Time-Dependent Phenomena. *Top. Curr. Chem.* **1996**, *181*, 81−172.
(29) *Electronic Density Functional Theory. Recent Progress and New Directions*; Dobson, J. F., Vignale, G., Das, M. P., Ed.; Plenum: New York, 1998.
(30) Marques, M. A. L.; Gross, E. K. U. Time-Dependent Density Functional Theory. *Annu. Rev. Phys. Chem.* **2004**, *55*, 427−455.
(31) Barron, L. D. *Molecular Light Scattering and Optical Activity*; Barron, L. D., Ed.; Cambridge University Press: New York, 2004.
(32) Olsen, J.; Jørgensen, P. Linear and Nonlinear Response Functions for an Exact State and for an MCSCF State. *J. Chem. Phys.* **1985**, *82*, 3235−3264.
(33) Norman, P.; Bishop, D. M.; Jensen, H. J. Aa.; Oddershede, J. Near-Resonant Absorption in the Time-Dependent Self-Consistent Field and Multiconfigurational Self-Consistent Field Approximations. *J. Chem. Phys.* **2001**, *115*, 10323−10334.
(34) Jensen, L.; Autschbach, J.; Schatz, G. C. Finite Lifetime Effects on the Polarizability within Time-Dependent Density-Functional Theory. *J. Chem. Phys.* **2005**, *122*, 224115.
(35) Jensen, L.; Åstrand, P.-O.; Mikkelsen, K. V. Molecular Mechanics Interaction Models for Optical Electronic Properties. *J. Comput. Theor. Nanosci.* **2009**, *6*, 270−291.
(36) Smalø, H. S.; Åstrand, P.-O.; Mayer, A. Combined Nonmetallic Electronegativity Equalisation and Point-Dipole Interaction Model for the Frequency-Dependent Polarisability. *Mol. Phys.* **2013**, *111*, 1470−1481.
(37) Smalø, H. S.; Åstrand, P.-O.; Jensen, L. Nonmetallic Electronegativity Equalization and Point-Dipole Interaction Model Including Exchange Interactions for Molecular Dipole Moments and Polarizabilities. *J. Chem. Phys.* **2009**, *131*, 044101.
(38) Mayer, A.; Lambin, P.; Åstrand, P.-O. An Electrostatic Interaction Model for Frequency-Dependent Polarizability: Methodology and Applications to Hydrocarbons and Fullerenes. *Nanotechnology* **2008**, *19*, 025203.
(39) Mortier, W. J.; van Genechten, K.; Gasteiger, J. Electronegativity Equalization: Applications and Parametrization. *J. Am. Chem. Soc.* **1985**, *107*, 829−835.
(40) Stern, H. A.; Kaminski, G. A.; Banks, J. L.; Zhou, R.; Berne, B. J.; Friesner, R. A. Fluctuating Charge, Polarizable Dipole, and Combined Models: Parameterization from Ab Initio Quantum Chemistry. *J. Phys. Chem. B* **1999**, *103*, 4730−4737.
(41) Chelli, R.; Procacci, P.; Righini, R.; Califano, S. Electrical Response in Chemical Potential Equalization Schemes. *J. Chem. Phys.* **1999**, *111*, 8569−8575.
(42) Jensen, L.; Åstrand, P.-O.; Mikkelsen, K. V. An Atomic Capacitance-Polarizability Model for the Calculation of Molecular Dipole Moments and Polarizabilities. *Int. J. Quantum Chem.* **2001**, *84*, 513−522.
(43) Rick, S. W.; Stuart, S. J.; Berne, B. J. Dynamical Fluctuating Charge Force Fields: Application to Liquid Water. *J. Chem. Phys.* **1994**, *101*, 6141−6156.
(44) Shanker, B.; Applequist, J. Atom Monopole-Dipole Interaction Model with Limited Delocalization Length for Polarizabilities of Polyenes. *J. Phys. Chem.* **1996**, *100*, 10834−10836.
(45) Nistor, R. A.; Polihronov, J. G.; Müser, M. H.; Mosey, N. J. A Generalization of the Charge Equilibration Method for Nonmetallic Materials. *J. Chem. Phys.* **2006**, *125*, 094108.
(46) Mathieu, D. Split Charge Equalization Method with Correct Dissociation Limit. *J. Chem. Phys.* **2007**, *127*, 224103.
(47) Chen, J.; Martínez, T. J. QTPIE: Charge Transfer with Polarization Current Equalization. A Fluctuating Charge Model with Correct Asymptotics. *Chem. Phys. Lett.* **2007**, *438*, 315−320.
(48) Lee Warren, G.; Davis, J. E.; Patel, S. Origin and Control of Superlinear Polarizability Scaling in Chemical Potential Equalization Methods. *J. Chem. Phys.* **2008**, *128*, 144110.
(49) Chen, J.; Hundertmark, D.; Martínez, T. J. A Unified Theoretical Framework for Fluctuating-Charge Models in Atom-Space and in Bond-Space. *J. Chem. Phys.* **2008**, *129*, 214113.
(50) Nistor, R. A.; Müser, M. H. Dielectric Properties of Solids in the Regular and Split-Charge Equilibration Formalisms. *Phys. Rev. B* **2009**, *79*, 104303.
(51) Verstraelen, T.; Speybroeck, V. V.; Waroquier, M. The Electronegativity Equalization and the Split Charge Equilibration Applied to Organic Systems: Parametrization, Validation, and Comparison. *J. Chem. Phys.* **2009**, *131*, 044127.
(52) Ghosh, S. K. A Coarse-Grained Density Functional Theory, Chemical Potential Equalization and Electric Response in Molecular Systems. *J. Mol. Struct.: THEOCHEM* **2010**, *943*, 178−182.
(53) Bodrenko, I. V.; Della Salla, F. A Periodic Charge-Dipole Electrostatic Model. II. A Kinetic-Exchange-Correlation Correction. *J. Chem. Phys.* **2013**, *139*, 144109.
(54) Valone, S. M. Quantum Mechanical Origins of the Iczkowski-Margrave Model of Chemical Potential. *J. Chem. Theory Comput.* **2011**, *7*, 2253−2261.
(55) Verstraelen, T.; Ayers, P. W.; Van Speybroeck, V.; Waroquier, M. ACKS2: Atom-Condensed Kohn-Sham DFT Approximated to Second Order. *J. Chem. Phys.* **2013**, *138*, 074108.
(56) Silberstein, L. Molecular Refractivity and Atomic Interaction. *Philos. Mag.* **1917**, *33*, 92−128.
(57) Silberstein, L. Molecular Refractivity and Atomic Interaction. II. *Philos. Mag.* **1917**, *33*, 521−531.
(58) Applequist, J. An Atom Dipole Interaction Model for Molecular Optical Properties. *Acc. Chem. Res.* **1977**, *10*, 79−85.
(59) Applequist, J.; Carl, J. R.; Fung, K. F. An atom Dipole Interaction Model for Molecular Polarizability. Application to Polyatomic Molecules and Determination of Atom Polarizabilities. *J. Am. Chem. Soc.* **1972**, *94*, 2952−2960.
(60) Applequist, J. A Multipole Interaction Theory of Electric Polarization of Atomic and Molecular Assemblies. *J. Chem. Phys.* **1985**, *83*, 809−826; **1993**, *98*, 7664(E).
(61) Jensen, L.; Schmidt, O. H.; Mikkelsen, K. V.; Åstrand, P.-O. Static and Frequency-Dependent Polarizability Tensors for Carbon Nanotubes. *J. Phys. Chem. B* **2000**, *104*, 10462−10466.
(62) Kongsted, J.; Osted, A.; Jensen, L.; Åstrand, P.-O.; Mikkelsen, K. V. Frequency-Dependent Polarizability of Boron Nitride Nanotubes: A Theoretical Study. *J. Phys. Chem. B* **2001**, *105*, 10243−10248.
(63) Hansen, T.; Jensen, L.; Åstrand, P.-O.; Mikkelsen, K. V. Frequency-Dependent Polarizabilities of Amino Acids as Calculated by an Electrostatic Interaction Model. *J. Chem. Theory Comput.* **2005**, *1*, 626−633.
(64) Sundberg, K. R. A Group-Dipole Interaction Model of the Molecular Polarizability and the Molecular First and Second Hyperpolarizabilities. *J. Chem. Phys.* **1977**, *66*, 114−118.
(65) Buckingham, A. D.; Concannon, E. P.; Hands, I. D. Hyperpolarizability of Interacting Atoms. *J. Phys. Chem.* **1994**, *98*, 10455−10459.
(66) Jensen, L.; Sylvester-Hvid, K. O.; Mikkelsen, K. V.; Åstrand, P.-O. A Dipole Interaction Model for the Molecular Second Hyperpolarizability. *J. Phys. Chem. A* **2003**, *107*, 2270−2276.
(67) Jensen, L.; Åstrand, P.-O.; Mikkelsen, K. V. Saturation of the Third-Order Polarizability of Carbon Nanotubes Characterized by a Dipole Interaction Model. *Nano Lett.* **2003**, *3*, 661−665.
(68) Jensen, L.; Åstrand, P.-O.; Mikkelsen, K. V. Microscopic and Macroscopic Polarization in C_{60} Fullerene Clusters as Calculated by an Electrostatic Interaction Model. *J. Phys. Chem. B* **2004**, *108*, 8226−8233.
(69) Jensen, L.; Åstrand, P.-O.; Mikkelsen, K. V. The Static Polarizability and Second Hyperpolarizability of Fullerenes and Carbon Nanotubes. *J. Phys. Chem. A* **2004**, *108*, 8795−8800.

(70) Jensen, L.; Esbensen, A. L.; Åstrand, P.-O.; Mikkelsen, K. V. Microscopic Polarization in Ropes and Films of Aligned Carbon Nanotubes. *J. Comput. Meth. Sci. Eng.* **2006**, *6*, 353−564.
(71) Applequist, J. On the Polarizability Theory of Optical Rotation. *J. Chem. Phys.* **1973**, *58*, 4251−4259.
(72) Applequist, J. Optical Rotations of Cyclohexanepolyols from Polarizability Theory. *J. Am. Chem. Soc.* **1973**, *95*, 8258−8262.
(73) Sundberg, K. R. An Atom-Dipole Interaction Theory of the Hyperpolarizability Contribution to the Optical Activity in Molecules. *J. Chem. Phys.* **1978**, *68*, 5271−5276.
(74) Applequist, J. Comment on the Validity of the Atom Monopole-Dipole Interaction Model for Optical Activity. *J. Phys. Chem. A* **1998**, *102*, 7723−7724.
(75) Applequist, J.; Quicksall, C. O. Calculation of Raman Scattering Parameters for Methane and Halomethanes from an Atom Dipole Interaction Model. *J. Chem. Phys.* **1977**, *66*, 3455−3459.
(76) Bocian, D. F.; Schick, G. A.; Birge, R. R. Calculation of Raman Intensities for the Ring-Puckering Vibrations of Trimethylene Oxide and Cyclobutane. The Importance of Electrical Anharmonicity. *J. Chem. Phys.* **1981**, *74*, 3660−3667.
(77) Stern, H. A.; Rittner, F.; Berne, B. J.; Friesner, R. A. Combined Fluctuating Charge and Polarizable Dipole Models: Application to a Five-Site Water Potential Function. *J. Chem. Phys.* **2001**, *115*, 2237−2251.
(78) Mayer, A. Polarization of Metallic Carbon Nanotubes from a Model that Includes both Net Charges and Dipoles. *Phys. Rev. B* **2005**, *71*, 235333.
(79) Mayer, A. A Monopole-Dipole Model to Compute the Polarization of Metallic Carbon Nanotubes. *Appl. Phys. Lett.* **2005**, *86*, 153110.
(80) Mayer, A.; Lambin, P.; Langlet, R. Charge-Dipole Model to Compute the Polarization of Fullerenes. *Appl. Phys. Lett.* **2006**, *89*, 063117.
(81) Mayer, A. Formulation in Terms of Normalized Propagators of a Charge-Dipole Model Enabling the Calculation of the Polarization Properties of Fullerenes and Carbon Nanotubes. *Phys. Rev. B* **2007**, *75*, 045407.
(82) Mayer, A.; Åstrand, P.-O. A Charge-Dipole Model for the Static Polarizability of Nanostructures Including Aliphatic, Olephinic, and Aromatic Systems. *J. Phys. Chem. A* **2008**, *112*, 1277−1285.
(83) Olson, M. L.; Sundberg, K. R. An Atom Monopole-Dipole Interaction Model with Charge Transfer for the Treatment of Polarizabilities of π-Bonded Molecules. *J. Chem. Phys.* **1978**, *69*, 5400−5404.
(84) Applequist, J. Atom Charge Transfer in Molecular Polarizabilities. Application of the Olson-Sundberg Model to Aliphatic and Aromatic Hydrocarbons. *J. Phys. Chem.* **1993**, *97*, 6016−6023.
(85) Shanker, B.; Applequist, J. Polarizabilities of Fullerenes C_{20} through C_{240} from Atom Monopole-Dipole Interaction Theory. *J. Phys. Chem.* **1994**, *98*, 6486−6489.
(86) Jensen, L. L.; Jensen, L. Electrostatic Interaction Model for the Calculation of the Polarizability of Large Noble Metal Nanoclusters. *J. Phys. Chem. C* **2008**, *112*, 15697−15703.
(87) Bakowies, D.; Thiel, W. Hybrid Models for Combined Quantum Mechanical and Molecular Mechanical Approaches. *J. Phys. Chem.* **1996**, *100*, 10580−10594.
(88) Jensen, L.; Åstrand, P.-O.; Osted, A.; Kongsted, J.; Mikkelsen, K. V. Polarizability of Molecular Clusters as Calculated by a Dipole Interaction Model. *J. Chem. Phys.* **2002**, *116*, 4001−4010.
(89) Ponǵratz, A.; Markǵraf, G.; Maier-Pitsch, E. Über Absorptionsspektren Einiger Parasubstituierter Azobenzol-Abkömmlinge ein Beitrag zur Dilthey-Wizingerschen Chromophortheorie. *Ber. Dtsch. Chem. Ges.* **1938**, *71*, 1287−1296.
(90) Buttingsrud, B.; Alsberg, B. K.; Åstrand, P.-O. Quantitative Prediction of the Absorption Maxima of Azobenzene Dyes from Bond Lengths and Critical Points in the Electron Density. *Phys. Chem. Chem. Phys.* **2007**, *9*, 2226−2233.
(91) Thole, B. T. Molecular Polarizabilities Calculated with a Modified Dipole Interaction. *Chem. Phys.* **1981**, *59*, 341−350.
(92) Birge, R. R.; Schick, G. A.; Bocian, D. F. Calculation of Molecular Polarizabilities Using a Semiclassical Slater-Type Orbital-Point Dipole Interaction (STOPDI) model. *J. Chem. Phys.* **1983**, *79*, 2256−2264.
(93) Rappé, A. K.; Goddard, W. A., III Charge Equilibration for Molecular Dynamics Simulations. *J. Phys. Chem.* **1991**, *95*, 3358−3363.
(94) York, D. M.; Yang, W. A Chemical Potential Equalization Method for Molecular Simulations. *J. Chem. Phys.* **1996**, *104*, 159−172.
(95) Chelli, R.; Procacci, P. A Transferable Polarizable Electrostatic Force Field for Molecular Mechanics Based on the Chemical Potential Equalization Principle. *J. Chem. Phys.* **2002**, *117*, 9175−9189.
(96) van der Velde, G. A. A Realistic Coulomb Potential. *MD and MC on Water*; Berendsen, H. J. C., Ed.; CECAM: France, 1972.
(97) Buckingham, A. D. Permanent and Induced Molecular Moments and Long-Range Intermolecular Forces. *Adv. Chem. Phys.* **1967**, *12*, 107−142.
(98) te Velde, G.; Bickelhaupt, F. M.; van Gisbergen, S. J. A.; Fonseca Guerra, C.; Baerends, E. J.; Snijders, J. G.; Ziegler, T. Chemisty with ADF. *J. Comput. Chem.* **2001**, *22*, 931−967.
(99) Fonseca Guerra, C.; Snijders, J. G.; te Velde, G.; Baerends, E. J. Towards an Order-*N* DFT Method. *Theor. Chem. Acc.* **1998**, *99*, 391−401.
(100) ADF2010, *SCM, Theoretical Chemistry*; Vrije Universiteit: Amsterdam, The Netherlands; http://www.scm.com.
(101) Perdew, J. P.; Burke, K.; Ernzerhof, M. Generalized Gradient Approximation Made Simple. *Phys. Rev. Lett.* **1996**, *77*, 3865−3868.
(102) van Lenthe, E.; Baerends, E. J. Optimized Slater-Type Basis Sets for the Elements 1−118. *J. Comput. Chem.* **2003**, *24*, 1142−1156.
(103) Chong, D. P. Augmenting Basis Set for Time-Dependent Density Functional Theory Calculation of Excitation Energies: Slater-Type Orbitals for Hydrogen to Krypton. *Mol. Phys.* **2005**, *103*, 749−761.
(104) Jensen, L.; Zhao, L.; Autschbach, J.; Schatz, G. C. Theory and Method for Calculating Resonance Raman Scattering from Resonance Polarizability Derivatives. *J. Chem. Phys.* **2005**, *123*, 174110.
(105) Verstraelen, T.; Bultinck, P.; Van Speybroeck, V.; Ayers, P. W.; Van Neck, D.; Waroquier, M. The Significance of Parameters in Charge Equilibration Models. *J. Chem. Theory Comput.* **2011**, *7*, 1750−1764.
(106) Kannemann, F. O.; Becke, A. D. Atomic Volumes and Polarizabilities in Density-Functional Theory. *J. Chem. Phys.* **2012**, *136*, 034109.
(107) Schubert, W. M.; Murphy, R. B.; Robins, J. Electron Donor and Acceptor Properties of Alkyl Substituents. *Tetrahedron* **1962**, *17*, 199−214.
(108) Politzer, P.; Abrahamsen, L.; Sjoberg, P. Effects of Amino and Nitro Substituents upon the Electrostatic Potential of an Aromatic Ring. *J. Am. Chem. Soc.* **1984**, *106*, 855−860.
(109) Goddard, W. A., III; Brenner, D. W.; Lyshevski, S. E.; Iafrate, G. J *Handbook of Nanoscience, Engineering, and Technology*; CRC Press: Boca Raton, FL, 2010; pp 7−54.
(110) Sylvester-Hvid, K. O.; Åstrand, P.-O.; Ratner, M. A.; Mikkelsen, K. V. Frequency-Dependent Molecular Polarizability and Refractive Index: Are Substituent Contributions Additive? *J. Phys. Chem. A* **1999**, *103*, 1818−1821.
(111) Lorentzon, J.; Malmqvist, P.-Å.; Fülscher, M.; Roos, B. O. A CASPT2 Study of the Valence and Lowest Rydberg Electronic States of Benzene and Phenol. *Theor. Chim. Acta.* **1995**, *91*, 91−108.
(112) Sawicki, E. Physical Properties of Aminoazobenzene Dyes. VII. Absorption Spectra 4-Aminoazobenzene Dyes in Ethanol. *Org. Chem.* **1957**, *22*, 915−919.
(113) Yagupolśkij, L. M.; Gandelśman, L. Z. The Effect of Substituents on the Color of N,N-Dialkylamino Azo Dyes and their Salts. *Zh. Obshch. Khim.* **1965**, *35*, 1252−1262.
(114) Haessner, C.; Mustroph, H. Untersuchungen zum UV/Vis-Spektralverhalten von Azofarbstoffen. XVIII. Substituenteneinflusse auf die Absorptionsmaxima der $n \rightarrow \pi^*$ und $\pi \rightarrow \pi^*$ -Banden von 4-N,N-Diethylaminoazobenzenen. *J. f. prakt. Chem.* **1987**, *329*, 493−498.

(115) Gerson, F.; Heilbronner, E. Physikalisch-Chemische Eigenschaften und Elektronenstruktur der Azo-Verbindungen. Teil XI: Bemerkung zur Struktur des Azonium-Kations des *p*, *p*′-Bis-Dimethylamino-Azobenzols. *Helv. Chim. Acta* **1962**, *45*, 51−59.
(116) Gerson, F.; Heilbronner, E. Physikalisch-Chemische Eigenschaften und Elektronenstruktur der Azo-Verbindungen. Teil X: Über die Protonierung der Azo-Gruppe in *p*′ - oder *m*′-Substituierten Derivaten des *p*-Dimethylamino-Azobenzols. *Helv. Chim. Acta* **1962**, *45*, 42−50.
(117) Griffiths, J.; Roozpeikar, B. Synthesis and Electronic Absorption Spectra of Dicyano-Derivatives of 4-Diethylaminoazobenzene. *J. Chem. Soc., Perkin Trans. I* **1976**, 42−45.